

Journal of  
**Applied Remote Sensing**

**Comprehensive analysis of new  
near-infrared avalanche photodiode  
structure**

Krzysztof Czuba  
Jarosław Jureńczyk  
Janusz Kaniewski

# Comprehensive analysis of new near-infrared avalanche photodiode structure

Krzysztof Czuba,\* Jaroslaw Jureńczyk, and Janusz Kaniewski

Institute of Electron Technology, Department of Photonics, Al. Lotnikow 32/46,  
Warsaw, 02-668 Poland

**Abstract.** The essential steps in simulations of modern separate absorption, grading, charge, and multiplication avalanche photodiode and their results are discussed. All simulations were performed using two commercial technology computer-aided design type software packages, namely Silvaco ATLAS and Crosslight APSYS. Comparison between those two frameworks was made and differences between them were pointed out. Several examples of the influence of changes made in individual layers on overall device characteristics have been shown. Proper selection of models and their parameters as well as its significance on results has been illustrated. Additionally, default values of material parameters were revised and adequate values from the literature were entered. Simulated characteristics of optimized structure were compared with ones obtained from measurements of real devices (e.g., current-voltage curves). Finally, properties of crucial layers in the structure were discussed. © The Authors. Published by SPIE under a Creative Commons Attribution 3.0 Unported License. Distribution or reproduction of this work in whole or in part requires full attribution of the original publication, including its DOI. [DOI: [10.1117/1.JRS.8.084999](https://doi.org/10.1117/1.JRS.8.084999)]

**Keywords:** separated absorption, grading, charge, and multiplication avalanche photodiode; near-infrared detectors; simulations; InGaAs.

Paper 13491SS received Nov. 29, 2013; accepted for publication Jan. 15, 2014; published online Feb. 19, 2014.

## 1 Introduction

Presently, near-infrared (NIR) regime of wavelength, from 0.75 to  $\sim 3 \mu\text{m}$ , is undoubtedly very important in many modern technologies. Probably, the best example of one such technology is fiber-optic communication, which makes use of the so-called transmission windows. Those are spectral subranges of very low optical attenuation in the short-wavelength IR range, for this particular case in silica glass.

Working in NIR range requires both efficient light sources and good photodetectors, for which values of important figures of merit fulfill the requirements of specific application. Continuous improvement of parameters in these types of semiconductor devices is possible because of significant progress in three main fields. First of them is the development of material technology, namely, materials of better quality can be obtained by new emerging methods and/or by perfecting those already utilized. Second is to search and try to create new compound semiconductors that are usually directly related to the above-mentioned techniques. Finally, one could complicate the structure of the device itself so that better parameters could be achieved. Aforementioned areas are naturally interconnected, thus opening completely new possibilities in the design process of a device.

The avalanche photodiode is a very good example of a semiconductor device that underwent dynamic changes over the last 40 years. First structures were made by using silicon technology, well known at that time, and were used almost entirely in telecommunication applications. Industry was mainly concerned with optimization of the structure, so that maximum bandwidth could be further increased. Hence, achieving higher throughput and faster information exchange was possible. Thanks to their internal gain, avalanche photodiodes (APDs) very quickly started to replace devices used up until then in many applications, e.g., photomultipliers. Rapid

---

\*Address all correspondence to: Krzysztof Czuba, [kczuba@ite.waw.pl](mailto:kczuba@ite.waw.pl)

development of this type of detectors allows them to be applied in many diverse areas, e.g., optical radars, astronomy, medicine, spectroscopy, telecommunication, etc.<sup>1</sup>

The process of designing such complicated modern devices as APDs requires deep understanding of semiconductor physics. However, even in such cases, it is very difficult to predict overall properties of the structure. Modern technology can be helpful in designing photodiodes via more and more sophisticated simulation software with many numerical models of physical phenomena implemented. This type of software package belongs to a category defined as technology computer-aided design (TCAD). TCAD, as its name suggests, can significantly lower the costs of technology involved. Simultaneously, one can deepen the knowledge of physical processes existing in considered structures by detailed analysis of obtained results.

## 2 Structure

Novel applications require modern structures of APD, often with very specific properties. A response to the growing industrial and scientific demands is, for example, a structure with separated absorption, grading, charge, and multiplication regions (SAGCM). In this paper, the structure of one such device has been considered and its details are presented in Table 1 (from now on the structure in Table 1 is referred to as basic structure). It was considered a basis for all modifications described in the following sections.

In this type of photodetector, the structure consists of independent to large extent layers, which serve different functions. This type of construction leads to significant improvement in operating parameters of photodiodes. An unquestionable advantage of separated regions design is the possibility to influence output properties through adequate modifications of specific regions.

The basic structure was inspired by the device proposed by Li.<sup>2</sup> The materials used to fabricate photodiodes were selected so that the lattice constant would be matched to InP substrates. This results in elimination of the strain, which would otherwise cause major side effects. The absorber region and contact layer were made of ternary  $\text{In}_{0.53}\text{Ga}_{0.47}\text{As}$ , which is characterized by a small band gap allowing for absorption of radiation with a wavelength of  $\sim 1.55 \mu\text{m}$ . The rest of epitaxial layers are made of  $\text{In}_{0.52}\text{Al}_{0.48}\text{As}$ , characterized by a band gap slightly larger than that of a substrate. It significantly suppresses the effects related to

**Table 1** Structure of separated absorption, grading, charge, and multiplication avalanche photodiode.

Layer	Material	Doping type	Doping concentration ( $\text{cm}^{-3}$ )	Thickness (nm)
Contact	$\text{In}_{0.53}\text{Ga}_{0.47}\text{As}$	p	$1 \times 10^{19}$	50
Barrier	$\text{In}_{0.52}\text{Al}_{0.48}\text{As}$	p	$1 \times 10^{19}$	200
Absorber	$\text{In}_{0.53}\text{Ga}_{0.47}\text{As}$	p	$2.5 \times 10^{18}$	150
	$\text{In}_{0.53}\text{Ga}_{0.47}\text{As}$	p	$1 \times 10^{18}$	150
	$\text{In}_{0.53}\text{Ga}_{0.47}\text{As}$	p	$4 \times 10^{17}$	150
Grading	$\text{In}_{0.5310.52}\text{Ga}_{0.4710}\text{Al}_{0.48}\text{As}$	i	$1 \times 10^{15}$	50
Separation	$\text{In}_{0.52}\text{Al}_{0.48}\text{As}$	i	$1 \times 10^{15}$	100
Charge	$\text{In}_{0.52}\text{Al}_{0.48}\text{As}$	p	$4 \times 10^{17}$	90
Multiplication	$\text{In}_{0.52}\text{Al}_{0.48}\text{As}$	i	$1 \times 10^{15}$	150
Buffer	$\text{In}_{0.52}\text{Al}_{0.48}\text{As}$	n	$5 \times 10^{18}$	800
Substrate	InP		Semi-insulating	$1.1 \times 10^6$

the Auger and the Shockley–Read–Hall (SRH) processes. Consequently, it results in the reduction of the dark current flowing through the structure. In addition, intrinsic layer of this material was used for avalanche multiplication of generated carriers. There is also a transition layer, situated between the separating and the absorption layers, which allows for as continuous and smooth as possible variation of the energy band edges at the interface between two different materials. This kind of procedure eliminates discontinuities at the heterointerface and accumulation of holes.<sup>3</sup> The latter considerably improves the transport parameters of optically generated carriers. A particular feature of the simulated construction is that the radiation absorbing region is separated from the multiplication area. Hence, no excessive generation of electron-hole pairs due to electric field rather than optical absorption would occur. Absorber thickness was chosen to be a few times lower than the average diffusion length of an electron in p-type  $\text{In}_{0.53}\text{Ga}_{0.47}\text{As}$ . It significantly increases a probability of effective collection of generated carriers. The doping of the absorber sublayers is made in such a way as to generate a small, built-in electric field, which aids electron flow in the proper direction. An additional barrier layer is located between the absorber and the contact layer and prevents flow of electrons from contact to device. This results in further suppression of dark current level. As was previously mentioned, generated carriers arrive into a high electric field region, where they are accelerated and signal is amplified via avalanche multiplication phenomena. Reduction of the breakdown voltage to relatively small values requires creating highly doped  $\text{p}^+\text{-i-n}^+$  junction. In this case, electric field of large magnitude spreads in layer situated between  $\text{p}^+$ -type charge and  $\text{n}^+$ -type buffer.<sup>4</sup> Multiplication process occurs in the intrinsic region via impact ionization of injected carriers.

Simulations of above-mentioned APD were performed in two software packages, which are described in the subsequent section.

### 3 Simulation Software and Models

Results presented in this paper were obtained by the use of two software packages, namely Crosslight APSYS and Silvaco ATLAS (ATLAS is an element of Silvaco TCAD software).<sup>5,6</sup> Both are, in general, defined by their developers as general-purpose simulators of optoelectronic devices. They have, however, different possibilities and limitations.

APSYS is a stand-alone, two-dimensional (2-D) finite element analysis and modeling program for simulating semiconductor devices. It provides a well-developed and modern graphical user interface. A number of physical models have been implemented to allow for simulation of many devices, such as transistor and photodetectors, except semiconductor lasers. The latter can be simulated by other Crosslight products. APSYS is capable of modeling electrical, optical, small signal, thermal, and transient characteristics, e.g., current-voltage curves, distributions of potential, electric field, and carrier concentrations, band structure, etc. The program solves, self-consistently, drift-diffusion, hydrodynamic, and heat transfer equations. It also provides additional features, such as hydrodynamic models for hot carriers, impact ionization models, thermionic emission for carriers transport in heterostructures, trap-related models, k-p model, low-temperature simulations, and more. Its internal database contains many parameters of materials, mainly silicon, and other compound semiconductors, but not all of them are properly described. There is, however, a possibility to implement one's own material models using C or Fortran syntax.

ATLAS is, similar to APSYS, a general-purpose, 2-D physically based simulation software with additional capabilities of operating in three dimensions. It is designed to work with interactive tools, which provide integrated development environment with graphical interface for inputs and postprocessing program to visualize results. Opposite to APSYS, ATLAS is capable of simulating a wider range of semiconductor devices. Additionally, far more models are implemented, including those developed only for specific devices. It uses various powerful numerical techniques, which can be chosen depending on the user's needs. ATLAS has the same capabilities as APSYS and more. For example, it allows for using arbitrary geometry of devices. Similar to Crosslight product, a material database has been implemented, but default values are not always accurate and their revision is often required. It is also possible to create one's own material models using C Interpreter.

From a computational point of view, ATLAS is a more modern software that effectively utilizes multicore and multithread architecture of processors as well as fast, high-capacity memory. It has no limits whatsoever in using available resources, which is completely different from APSYS.

In case of APD, following general models are required: carrier transport, impact ionization, tunneling, and recombination. Both software packages provide what is necessary but to a different degree. For carrier transport, standard drift-diffusion equations are used. Impact ionization is modeled with impact ionization coefficients method. However, different algorithms are implemented in each program. APSYS uses standard Chynoweth exponential dependence of ionization coefficients of electric field,<sup>7</sup> whereas ATLAS provides a multitude of local and nonlocal models. For the purposes of this paper, a local Selberherr model, which is in fact a variation of Chynoweth one, was used,<sup>8</sup> partly because of availability of parameters for InGaAs/InAlAs/InP material system. Tunneling in APSYS is described by Zener tunneling model. It is a local field dependent approximation of band-to-band tunneling that can be directly simultaneously incorporated into drift-diffusion calculations with impact ionization model. It requires direct bandgap semiconductor with both valence and conduction band maxima at point  $\Gamma$ . In ATLAS local and nonlocal band-to-band models were used. The former allows for performing quick calculations and is equivalent to APSYS Zener tunneling model. The latter improves accuracy of results by taking into account special variation of energy bands. Additionally, it accounts for the lack of spatial coincidence of generation and recombination processes of electron and holes. The way the nonlocal model is implemented in Silvaco's software makes it easier to simulate structures with complicated geometry. Recombination processes are, in general, described by the following three theories: Auger, SRH, bimolecular. In APSYS ratios of all of these are calculated from widely known equations containing proper recombination coefficients. ATLAS also provides such basic models; however, in addition, it allows for the use of more complicated temperature, carrier concentration dependent, and more models. In the case of simulated SAGCM APD, simple Auger and bimolecular recombination models were chosen. For SRH recombination, carrier concentration dependent relation was used, with data for materials taken from the literature.<sup>9</sup>

## 4 Results and Discussion

In this section, results obtained from measurements and simulations of SAGCM APD are presented and discussed. Band diagrams carry important information about basic operating mechanisms and allow for verification of correctness of the concept. In Fig. 1, band diagrams of SAGCM APD, at thermodynamic equilibrium, for basic structure are shown. These types of calculations require accurate data concerning affinity, bandgap, and band offsets for specific material system. Only then proper depiction of heterostructure and precise definition of band discontinuities on interfaces between subsequent layers is possible.

In Fig. 1 there are conduction and valence band edges obtained from ATLAS and APSYS software. Generally, the curves in both cases are very similar; however, there are some discrepancies. First, ATLAS calculated slightly smaller value of energy gap for  $\text{In}_{0.52}\text{Al}_{0.48}\text{As}$ , which can be observed in barrier, separating, charge, and buffer layers. It results from the use of different equations for such calculations as well as rounding of parameters. An analogous situation occurs for  $\text{InP}$  and  $\text{In}_{0.53}\text{Ga}_{0.47}\text{As}$ . At the interfaces of barrier and buffer layers, there are some discontinuities, which can be explained by not fine enough mesh. In spite of the aforementioned differences, both band diagrams are in agreement with predictions based on the information collected in Table 1.

In Fig. 2, dark current-voltage characteristics of SAGCM APD for three different concentrations in charge layer are shown. Significantly lower dark current levels obtained from ATLAS in comparison with those from APSYS were observed. This can be explained by two overlapping effects. At first both software packages have different default values of depth in 2-D simulations. ATLAS assumes that 2-D structure is  $1\ \mu\text{m}$  thick in third dimension, whereas APSYS uses 1 m instead. Second, utilization of nonidentical models, especially nonlocal ones in ATLAS, causes discrepancies in calculated values of dark current.

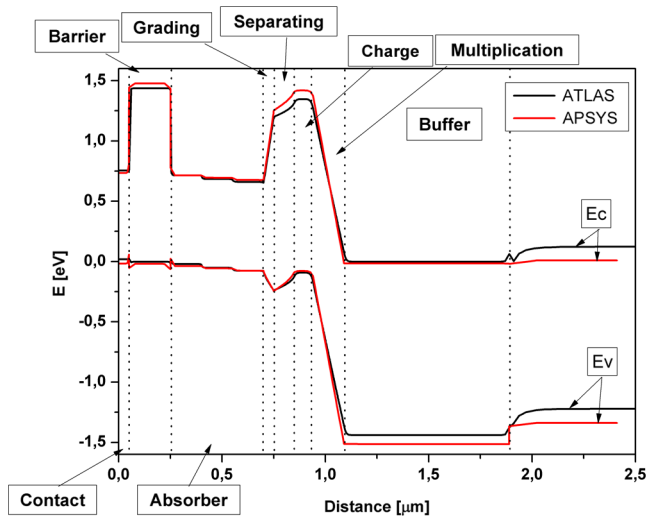


**Fig. 1** Band diagrams at thermodynamic equilibrium obtained using ATLAS (black line) and APSYS (red line).

Additionally, breakdown voltages for both groups of I-V curves are not the same. For basic structure, the difference in values of this figure of merit is  $\sim 3.6$  V. Similar trend is observed for other shown characteristics. It is a direct result of nonequal doping concentrations in multiplication layers and distinct impact ionization data for  $\text{In}_{0.52}\text{Ga}_{0.48}\text{As}$  in both frameworks. In case of ATLAS, intrinsic concentration in multiplication region was set to  $1 \times 10^{15} \text{ cm}^{-3}$ , whereas in APSYS, it is by default set to  $0 \text{ cm}^{-3}$ . Mentioned material parameters decide how fast impact ionization occurs as a function of electric field; thus, a very strong change of breakdown voltage is observed. The difference between characteristics from APSYS and ATLAS as well as breakdown voltage increases as doping concentration in charge layer decreases. However, despite all of this, the shape of the curves vary only slightly from one software package to another.

Next, analysis of electric field distribution in SAGCM APD structure was performed. It gives an answer to the question whether chosen doping concentrations and layer thicknesses assure proper operation of simulated device. In Fig. 3, cross-sectional electric field distribution, for basic structure, at breakdown is shown. Junction area can be clearly distinguished as the region with the highest magnitude of electric field. Differences between curves in multiplication region

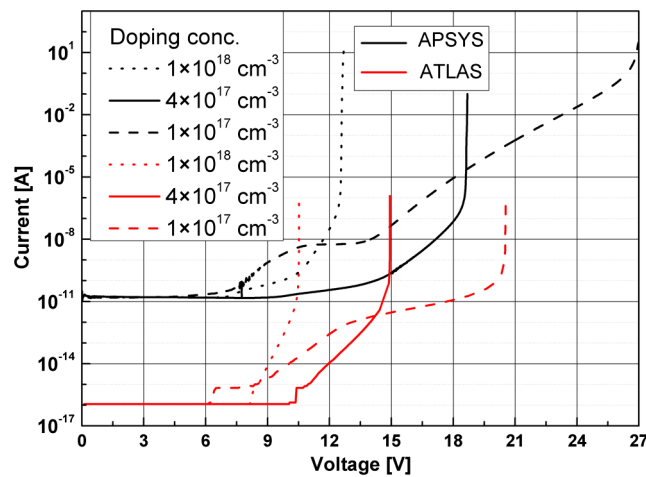


**Fig. 2** Dark current-voltage characteristics of the basic structure and two with modified doping concentration in charge layer.

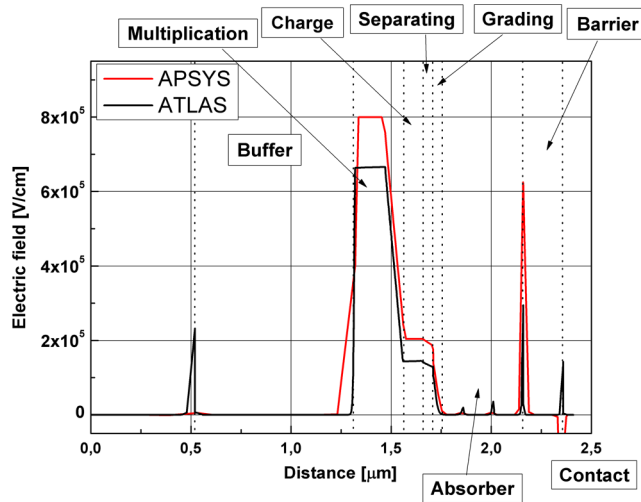


**Fig. 3** Electric field distribution through the basic structure at breakdown; curves obtained from APSYS (red line) and ATLAS (black line).

in Fig. 3 are consistent with those observed in Fig. 2. From comparison of these two figures, it is clear that there exists a direct correlation between magnitude of electric field in multiplication layer and breakdown voltage. Additionally, since electric field is dependent on differences in doping concentration in subsequent layers within junction, statements made in comment to Fig. 2 are still valid.

Both curves show that the electric field is confined to the area of the junction. Absorber is clearly undepleted, which is consistent with both the concept of separated regions photodiode and band diagram presented in Fig. 1. There is, however, a built-in electric field assuring unidirectional transport of photoelectrons, resulting from step-like doping distribution in this layer. It is indicated by peaks observed at interfaces between neighboring sublayers of different acceptor concentration. Such peaks can be seen between every two layers of different doping concentration and type. Their shape strongly depends on mesh density in the vicinity of interfaces.

An important part of the analysis is the comparison between simulated results and experimental data. In Fig. 4 dark [Fig. 4(a)] and light [Fig. 4(b)] current-voltage curves for simulated and measured APDs are shown. Dark current level is obviously much higher in real device as simulation requires many simplifications and measurement equipment has its limitations. In case of real photodetector, both growth and processing technology determine how much influence

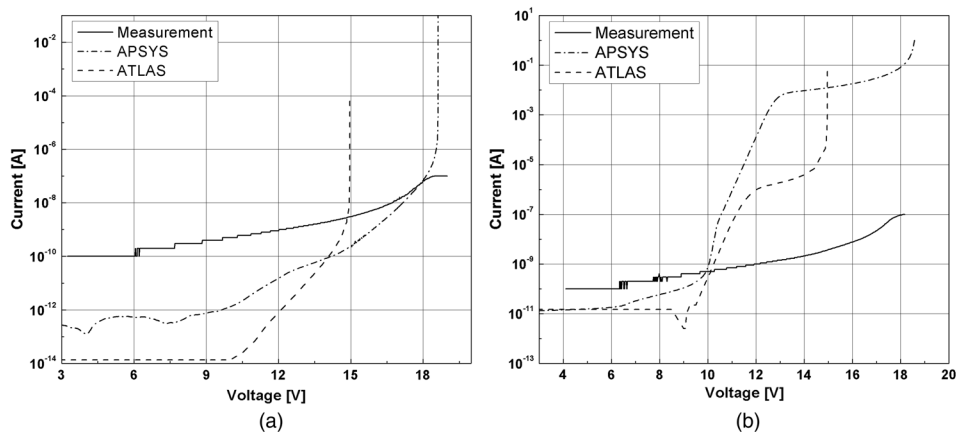


**Fig. 4** Comparison of current-voltage curves for basic structure between simulated and experimentally determined ones: (a) dark characteristics and (b) light characteristics.

factors such as abruptness of interfaces, uniformity of distribution of composition and doping, presence of defects, quality of metallic contacts, etc. have on dark current. Simulations and measurement were made for ambient temperature equal to 300 K, so there must be additional noise present in latter results.

Simulated light characteristics in Fig. 4(b) have very similar shape despite the fact of having different breakdown voltage values. Analogous to dark current, the light current level is higher in real photodiode. Measurement and simulations in ATLAS were performed for light source with irradiance of  $50 \mu\text{W cm}^{-2}$  (in case of measurement it is estimated value), whereas in APSYS irradiance was 10 times larger.

Generally speaking, the shape of the measured I-V curves is consistent with the simulated ones, especially those obtained from APSYS. Experimentally determined breakdown voltage appears to have values closer to the one obtained from Crosslight software. There are a few possible explanations for such behavior. One is the correspondence between material parameters implemented in APSYS and those of real device. Another one is that doping concentrations in charge and multiplication regions of real detector are less than ones given for basic structure. As a consequence, breakdown voltage would shift to higher values as mentioned in the description of Fig. 2. Similarly, any fluctuations of composition throughout specific layers also cause changes in material parameters.

Finally, simulated and measured spectral responses were compared. Unfortunately, numerical calculations of this kind were only possible in ATLAS software. In Fig. 5, normalized photo-response curves as a function of wavelength are shown. In both simulations and measurements light source parameters were identical to those mentioned before. There are clear differences in values of wavelengths corresponding to maximum response. This is a result of oversimplified model of radiation absorption in ATLAS. Generation rate depends only on extinction coefficient of material constituting absorption layer. Chosen models do not account for thermalization process of photogenerated carriers, which causes much more efficient absorption of photons with energy closer to the bandgap.

In case of measured curve, there is a discrepancy between obtained maximum response for wavelength of  $\sim 1.7 \mu\text{m}$  and expected  $1.55 \mu\text{m}$ . This can be explained as an effect of composition fluctuation in absorber. For wavelength of  $\sim 1 \mu\text{m}$ , there appears a peak in photoresponse. A similar response was observed in simulated curve, however, slightly shifted in the direction of lower frequencies. In case of modeled response, aforementioned peak disappeared with the exclusion of substrate from the structure. This suggests that additional optical effects, such as interference, can occur and modify spectral response.

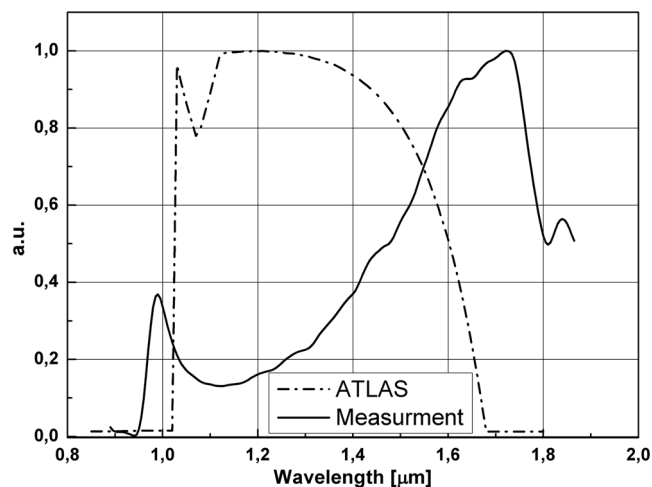


**Fig. 5** Measured and simulated spectral response of separated absorption, grading, charge, and multiplication avalanche photodiode.

## 5 Summary

Results of simulations and measurements of NIR SAGCM APD were presented and compared. Two commercially available TCAD software packages were used and their differences were pointed out. The influence of changes in specific layers on the output parameters of considered photodetector was demonstrated. Good agreement between simulation and measurement was found. However, in some cases, discrepancies were observed and resulted rather from oversimplification of used models than the correctness of method itself.

In conclusion, examples presented in this paper unequivocally indicate that numerical methods are necessary elements in the process of designing modern semiconductor devices.

## References

1. J. C. Campbell, "Recent advances in telecommunications avalanche photodiodes," *J. Lightwave Technol.* **25**(1), 109–121 (2007), <http://dx.doi.org/10.1109/JLT.2006.888481>.
2. N. Li, "High-output-power photodetectors for analog optical links and avalanche photodiodes with undepleted absorber," Ph.D. Thesis, The University of Texas Austin (2005).
3. Y. G. Xiao, Z. Q. Li, and Z. M. S. Li, "Dynamic drift-diffusion simulation of InP/InGaAs SAGCM APD," *Phys. Status Solidi C* **4**(5), 1641–1645 (2007), <http://dx.doi.org/10.1002/pssc.200674253>.
4. Y. G. Xio, Z. Q. Li, and L. Z. M. Simon, "Modeling of avalanche photodiodes by Crosslight APSYS," *Proc. SPIE* **6294**, 62940Z (2006), <http://dx.doi.org/10.1117/12.681189>.
5. Crosslight Inc., "Crosslight device simulation software—general description," 2008.12.
6. Silvaco Inc., "Silvaco ATLAS user's manual," 21 August 2012 <https://dynamic.silvaco.com/dynamicweb/jsp/downloads/DownloadManualsAction.do?req=silen-manuals&nm=atlas> (25 November 2013).
7. A. G. Chynoweth, "Ionization rates for electrons and holes in silicon," *Phys. Rev.* **109**(4), 1537–1540 (1958), <http://dx.doi.org/10.1103/PhysRev.109.1537>.
8. S. Selberherr, *Analysis and Simulation of Semiconductor Devices*, Springer-Verlag, New York (1984).
9. S. Masudy-Panah and M. K. Moravvej-Farshi, "Non-local impact ionization coefficients of submicron In<sub>0.52</sub>Al<sub>0.48</sub>As avalanche photodiodes," *Int. J. Electron.* **96**(4), 437–444 (2009), <http://dx.doi.org/10.1080/00207210802654430>.

Biographies of the authors are not available.